Photonirvachak

Springer

J. Indian Soc. Remote Sens. (June 2009) 37:201–214

RESEARCH ARTICLE

Satellite-based Analysis of the Role of Land Use/Land Cover and Vegetation Density on Surface Temperature Regime of Delhi, India

Yogesh Kant · B.D. Bharath · Javed Mallick · Clement Atzberger · Norman Kerle

Received: 22 February 2008 / Accepted : 28 February 2009

Keywords Land surface temperature · Vegetation density · Emissivity · MNF

Abstract The knowledge of the surface temperature is important to a range of issues and themes in earth sciences central to urban climatology, global environmental change and human-environment interactions. The study analyses land surface temperature (LST) estimation using temporal ASTER (Advanced Spaceborne Thermal Emission and Reflection Radiometer) datasets (day time and night time) over National Capital Territory Delhi using the surface emissivity information at pixel level. The spatial variations of LST over different land use/land cover (LU/LC) at day time and night time were analysed and relationship between the spatial distribution of LU/LC and vegetation density with LST was developed. Minimum noise fraction (MNF) was used for LU/LC classification which gave better accuracy than classification with original bands. The satellite derived emissivity values were found to be in good agreement with literature and field measured values. It was observed that fallow land, waste land/ bare soil, commercial/industrial and high dense built-up area have high surface temperature values during day time, compared to those over water bodies, agricultural cropland, and dense vegetation. During night time high surface temperature values are found over high dense built-up, water bodies, commercial/

Y. Kant[1] (✉) · B.D. Bharath[1] · J. Mallick[2] · C. Atzberger[3] · N. Kerle[4]
[1]Indian Institute of Remote Sensing (NRSC), ISRO, Govt. of India, 4 Kalidas Road, Dehradun – 248 001, India
[2]Geography Department, Jamia Millia Islamia University, New Delhi – 110 025, India
[3]Joint Research Centre (JRC) of the European Commission, MARS Unit, 21027, Ispra, Italy
[4]International Institute for Geo-Information Science and Earth Observation (ITC), Enschede, The Netherlands

email : ykanty@yahoo.com

industrial and low dense built-up than over fallow land, dense vegetation and agricultural cropland. It was found that there is a strong negative correlation between surface temperature and NDVI over dense vegetation, sparse vegetation and low dense built-up area while with fraction vegetation cover, it indicates a moderate negative correlation. The results suggest that the methodology is feasible to estimate NDVI, surface emissivity and surface temperature with reasonable accuracy over heterogeneous urban area. The analysis also indicates that the relationship between the spatial distribution of LU/LC and vegetation density is closely related to the development of urban heat islands (UHI).

Introduction

Land surface temperature is key in the studies related to the global environmental change, human-environment interactions, remote sensing based land surface modelling schemes (Kustas and Norman, 1996) and more specifically to urban climatology. Impact of urbanization leads to increase in surface temperature in urban areas mainly due to alteration of natural surfaces which affect the absorption of solar radiation, surface temperature, evaporation rates and can drastically alter the conditions of the near-surface atmosphere. The complexity of urban surfaces poses difficulty in obtaining representative measurements of surface temperature because of the number of surfaces that need to be sampled.

In remote sensing, Thermal infrared (TIR) sensors can obtain quantitative information on surface temperature across the LU/LC categories. There are many satellite based thermal infrared sensors available in the studies related to LST. The Geostationary Operational Environmental Satellite (GOES) has a 4 km resolution in the thermal infrared, while the NOAA-Advanced Very High Resolution Radiometer (AVHRR) and the Moderate Resolution Imaging Spectroradiometer (MODIS) have 1 km spatial resolution. In the category of high resolution is the Terra-Advanced Spaceborne Thermal Emission and Reflection Radiometer (ASTER) which has a 90 m spatial resolution and Landsat-7 Enhanced Thematic Mapper (ETM+) having 60 m resolution in thermal region. LST is sensitive to vegetation, soil moisture and it can be used to detect LU/LC changes, e.g. tendencies towards urbanization, desertification, etc.

In this study LST was analysed using temporal ASTER datasets (day time and night time) over heterogeneous urban area. ASTER datasets has been used to estimate the LST using the Temperature Emissivity Separation (TES) algorithm which uses the Normalised Emissivity Method (NEM) (Gillespie, 1985), from which emissivity ratios were computed. Accurate estimation of LST requires atmospheric correction of the satellite data and the estimation of surface emissivity (Gillespie *et al*., 1998; Schmugge *et al.*, 1998 and Wan *et al*., 2002). Validation for surface emissivity and LST was carried out using ground based measurements. The spatial variations of day and night time LST over different LU/LC were analysed and its relationship with the spatial distribution of LU/LC and vegetation density was developed.

Study area

Delhi is geographically situated between latitude 28^0 23' 17" – 28^0 53' 00" North and Longitude 76^0 50' 24" – 77^0 20' 37" East and lies at an altitude between 213 to 305 meters and covers an area of 1,483 km^2. It is situated on the bank of river Yamuna and borders in the east by the state of Uttar Pradesh and on the north, west, and south by the state of Haryana. Physiographically Delhi can be divided into three segments: the Yamuna flood plain, the ridge and the plain. The Yamuna flood plains are somewhat low-lying and sandy. The ridge constitutes the most

dominating physiographic features of this territory. It originates from the Aravali hills of Rajasthan, enters Delhi from the south and extends in a north-eastern direction. Rest of Delhi is categorized as a plain. The climate is markedly periodic and is characterized by dry and gradually increasing hot season between March and June, a dry and cold winter between October and February, and monsoon period between July and September. Wind is an important climatic factor for Delhi's environmental conditions. For most of the year, wind is mild with a mean velocity of 0.9 to 2 m/s. The vegetation in the ridge (forest) is predominately of thorny scrub type, which is usually found in arid and semi arid zone. Ridge Forest of Delhi falls in the category of 'Tropical thorn forest' as per the forest type classification of Champion and Seth (1968), and more especially as 'semi arid open scrub'. Among trees that are dominant are Acacias. Table 1 shows existing land use distribution in Delhi.

Table 1 Land use distribution of Delhi

Land use	Percentage of land
Residential	45–55
Commercial	3–4
Industrial	4–5
Green/Recreational	15–20
Public and semi-public facilities	8–10
Circulation	10–12

Source: Delhi Development Authority (DDA) Draft Master Plan, New Delhi.

As per Census 2001, National Capital Territory (NCT) Delhi had a population of 13.78 million and 46.28 per cent decennial population growth during 1991–2001. With the continuation of the present population trend, the total population of NCT Delhi by the year 2011 and 2021 would be around 18.2 million and 22.5 million respectively.

Satellite data processing

Temporal ASTER datasets of Delhi used in this study are :

- October 07, 2001 (Night time) of Path/row 13/204
- October 18, 2001 (Day time) of Path/row 146/40
- September 22, 2003 (Day time) of Path/row 146/40
- October 02, 2005 (Night time) of Path/row 13/204

ASTER has 14 bands of which bands 1–3 (0.52 –0.86 μm) have spatial resolution of 15m, bands 4 to 9 (1.60 –2.43 μm) have spatial resolution of 30 m and 5 thermal bands from band10 to14 (8.125–11.65 μm) have 90 m resolution.

Conversions from DN to spectral radiance of each band is done as follows:

$$L_\lambda = (DN - 1) \times UCC$$

The unit conversion coefficient (UCC) was used for different bands with gain settings (ASTER user Handbook).

Geometric and atmospheric correction

ASTER level-1B products are geometrically corrected data sets. For standardization ASTER 15 m (VNIR) data was compared with LANDSAT-7 ETM + 15 m data and it was noticed that geometrical accuracy was low. Also the GPS readings in the ground during pre-field campaign did not match with these locations. Hence there was need to further rectify and standardize all the ASTER datasets. All the images were geometrically rectified to a common Universal Transverse Mercator (UTM- WGS84) coordinate system and were resampled to their respective spatial resolution using the nearest-neighbour algorithm.

After applying the radiometric and geometric corrections, the subset images of radiance were created for the study area, both for visible and near

infrared bands of the ASTER datasets. Standard atmospheric and geometric parameters were estimated using the ENVI FLAASH (Fast line-of-sight atmospheric analysis of spectral hypercubes) software. The FLAASH models include a method for retrieving an estimated aerosol/haze amount from selected "dark" land pixels in the scene (Kaufman *et al.*, 1997). These parameters along with the geometric parameters for each of the images were used together for atmospheric correction.

Image classification

For image classification, pre-field visit was carried out during September 10–13, 2005 to have an idea of different LU/LC classes existing in the study area. Unsupervised classification was initially performed on ASTER datasets for an overall spectral separability of the LU/LC classes. A total of nine classes were considered to represent the major LU/LC of the study area namely: High dense built-up, Low dense built-up, Commercial/industrial area, Dense vegetation (forest), Sparse vegetation (including parks), Water bodies, Fallow land, Waste land/bare soil and Agricultural cropland.

An extensive field survey was carried out during October 3–8, 2005 using priori knowledge obtained from unsupervised classification to identify sample points in the imagery and ground truth collection. Based on the collected sample sets for respective LU/LC classes, training sets were selected in the FCC imagery to be used for supervised classification using Maximum likelihood classification (MLC) classification. Also measurements pertaining to emissivity and surface temperature on various LU/LC feature were taken using the emissivity box and infrared Thermometer.

MNF was performed on the ASTER data sets as to reduce the data redundancy and correlation between spectral bands. MNF was applied to VNIR bands of ASTER datasets. First three MNF components of ASTER data were used to classify the image using the MLC while the other components were discarded due to the higher proportion of noise content. In order to analyse the influence of the vegetation density on surface temperature, vegetation density component is derived using NDVI. The pixels with vegetation proportions along with NDVI could be used to compare and relate with surface temperature.

Emissivity and surface temperature measurement

Land surface emissivity is one of the important parameters in the studies related to energy balance. The emissivity is comparatively uniform for densely vegetated surfaces, whereas the emissivity over heterogeneous area is highly variable. However, it is possible to estimate the spectral emissivity variation for heterogeneous land using multi-spectral thermal infrared data.

TES algorithm is applied to Terra-ASTER data to compensate for reflected downwelling irradiance and to estimate the absolute spectral emissivity. The additional constraint to overcome the under-determination comes from the regression of the minimum emissivity of spectral contrast (calculated from laboratory spectra), used to equalize the number of unknowns and measurements, so that the set of Planck's equations for the measured thermal radiances can be inverted. In this study, five emissivity and one surface temperature maps were produced using the TES algorithm. Based on the above procedures, a detailed model was developed to automate the calculation of the Surface Temperature and five Emissivity maps.

Results

Analysis of land use/ land cover using ASTER data

Figure 1 shows the FCC image of two ASTER datasets of October 18, 2001 and September 22, 2003.

Residential areas (low and high dense built-up) in the central and eastern part and commercial/ industrial areas are better distinguishable in the MNF components than in FCC image. Commercial/ industrial areas are found in central part and in northern part of the image. Agricultural cropland areas are mostly in the north and north–eastern part of the image predominately with paddy and horticultural practices. Fallow lands and waste land/ bare soil were seen in the south and south western part of the image, dense vegetation (forest) in central and southern part of the image, sparse vegetation (including park and playgrounds) in central area and southern part of the image and small water bodies are seen towards northern part of the image. River Yamuna flows from north–east to south–east of the image. Thin canals are also seen flowing from north–east to south–west part of the image.

Supervised classification was carriedout using original bands and MNF components and it was observed that the classification improves using MNF components as compared to that using MLC. After examining the error matrix, it is found that there is a good improvement in the accuracies achieved with MNF. The overall classification accuracy for ASTER data of September 22, 2003 using MNF has been significantly improved to 86.81 % (kappa of 0.847) compared to MLC accuracy of 72.18% (kappa of 0.67) and 86.95% (kappa of 0.8509) for October 18, 2001 ASTER data as compared to MLC of 78.75% (kappa of 0.757). As the uncertainties observed in LU/LC considered is found to be lowest with MNF, classification with MNF components for all datasets has been considered.

Analysis of atmospheric correction

The radiance measured by the sensors may be affected depending on the prevailing atmospheric conditions at the time of satellite image acquisition. Hence, it is essential to consider the atmospheric effects and to apply the necessary atmospheric corrections to all the datasets. After applying the atmospheric correction to the ASTER datasets the dynamic range of NDVI has improved (from -0.234 to 0.575 over dense vegetation; -0.128 to 0.714 over agricultural cropland for dataset of September 22,

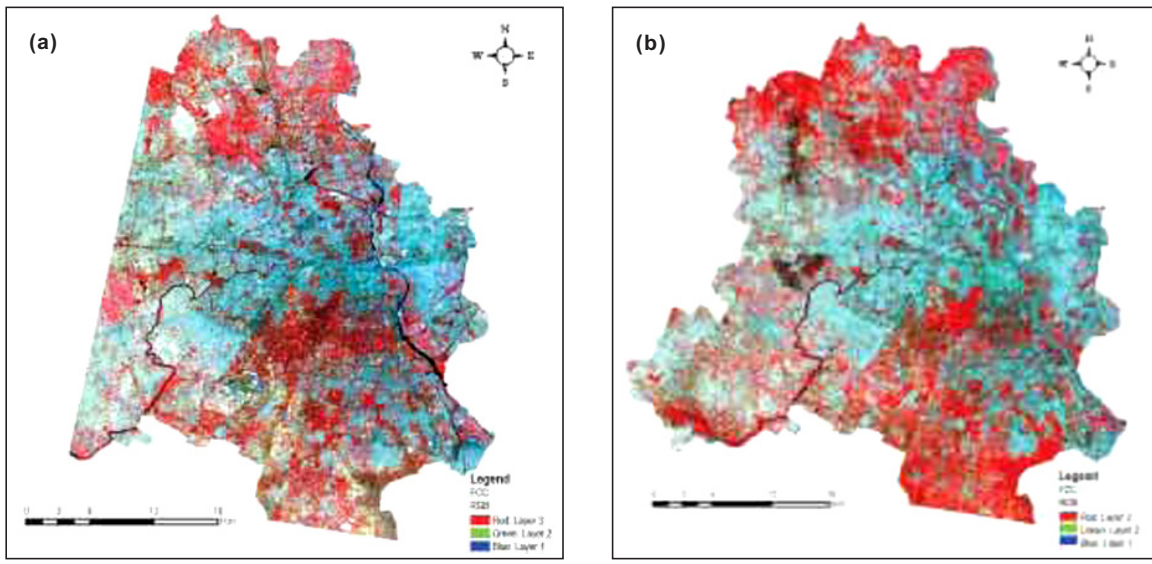

Fig. 1 ASTER False Colour Composite (FCC) image of Delhi, **(a)** October 18, 2001, **(b)** September 22, 2003.

2003). It was also seen in the improvement of overall dynamic range in NDVI values for other ASTER datasets. Similar atmospheric corrections have been applied for other datasets using FLAASH.

Analysis of vegetation density/vegetation abundance

The NDVI values are found in range of -0.059 to 0.633, having a mean value of 0.249 and standard deviation of 0.091 for October 18, 2001 and September 22, 2003 dataset. Higher NDVI values (bright areas) are observed in the central ridge, and north–west part of the image. Medium NDVI values (grey areas to bright areas) are observed over agricultural croplands (mainly paddy crop being dominant in the season) in the western and northern part of the image. Low NDVI values are seen over built-up areas and water bodies. A similar spatial distribution of vegetation is found in the fraction vegetation cover (FVC) image, with values in the range of 0 to 1 having a mean value of 0.196 and standard deviation of 0.131.

Table 2 shows the mean values of NDVI and vegetation fraction of two ASTER datasets of October 18, 2001 and September 22, 2003. The highest values are seen over agricultural cropland (paddy), followed by dense vegetation (forest) and lowest fraction vegetation value is over water bodies. Analysis between the NDVI and the fraction vegetation image shows a positive correlation (Pearson's correlation of 0.864 and 0.834 respectively for the two datasets) and correlation is significant at the level of 0.01 (1-tailed).

An attempt has been made to measure the emissivity using the emissivity box (Kant and Badarinath, 2002). All the measurements of temperature were done using TELATEMP infrared radiometer which operates in the 8–14 μm waveband with an instantaneous field of view (IFOV) of 2^o with an accuracy of 0.1^{o}C. The measurements were made using Emissivity box during October, 4–6, 2005 at various places taking different features of interest during the middle of sunny day when the stability of system is greater. This is achieved in the field by exposing the hot lid to direct solar radiation for 15 minutes so that the thermal equilibrium can be attained. To reduce the effect of noise in the final result, the value is taken after averaging over 10–15 successive measurements. The emissivity values presented here are the results of *in situ* measurements in and around Delhi area. The measurements could not be done on all the sample features of the area but only carriedout over some selected (dominant) features representing that LU/LC class. The measurements were carriedout on soil (for wasteland/bare soil), dense vegetation (*Prosopis*

Table 2 Statistics of NDVI and fraction vegetation cover of ASTER, October 18, 2001 and September 22, 2003

Land use/land cover	October 18, 2001				September 22, 2003			
	NDVI		Fraction cover		NDVI		Fraction cover	
	Mean	SD	Mean	SD	Mean	SD	Mean	SD
Dense vegetation (forest)	0.473	0.019	0.462	0.040	0.590	0.036	0.581	0.049
Sparse vegetation (grass/park)	0.356	0.038	0.365	0.081	0.467	0.062	0.373	0.027
Agricultural cropland (paddy)	0.499	0.026	0.677	0.122	0.625	0.051	0.722	0.049
Waste land / bare soil	0.157	0.015	0.072	0.027	0.137	0.021	0.084	0.011
Residential (low & dense built-up)	0.124	0.020	0.038	0.021	0.107	0.017	0.094	0.017
Water bodies	-0.0345	0.020	0.019	0.011	-0.047	0.023	0.035	0.002

juliflora, Bougainvillea in forest), sparse vegetation (grass, *Azadirachta indica* A. Jurr), agricultural crop (paddy), and urban (concrete, asphalt roads and sandstone). To determine the sample emissivity, the hot lid temperature must be higher than the sample temperature (15–20ºC) and remain constant during the time necessary for making L_1 and L_2 measurements. The emissivity measurement is rapidly made (within 2 minutes) in order that the temperature variation of the hot lid can be negligible, when it is introduced in the box. The value of the emissivities measured for soil and vegetation by the box method using the radiometer is shown in Table 3. It can be concluded that there is not much variation in emissivity values during the period of measurement. Hence, the average of the measurements can be taken as the values of the respective samples. The mean can be considered as a representative value that can be used in practice whereas standard deviations show the variability in emissivity values. The measured emisivity values were compared with those measured by Owe and Van de Griend, 1994 in Botswana campaign (tropical area) for bare soil in 8–14 μm region ($\varepsilon = 0.914$) which agrees well with the measured value over soil ($\varepsilon = 0.927$) and partly covered open grass ($\varepsilon = 0.949$) with the measured value over grass in parks ($\varepsilon = 0.9668$).

Analysis of land surface temperature and relationship with LU/LC

Figure 2 shows the spatial distribution of surface temperature using ASTER, dated September 22, 2003. The estimated LST ranges from 27.82 to 53.33°C (mean value being 35.83°C and standard deviation of 3.609). It is observed that in the image, west and south–west part of the study area exhibits maximum surface temperature due to fallow land and waste land/bare soil and the thermal gradient increases from built-up area (centre of image) to fallow land and wasteland (south–west of the image). Some high temperature pockets are also seen in central part of image. Water bodies exhibit low surface temperature values (ranges from 27.96 to 32.86°C). Vegetated areas, agricultural cropland has values from 28.93 to 32.94°C as compared to dense vegetation and sparse vegetation (ranges from 29.57 to 35.02°C). This may be due to the fact that surface temperature (crop temperature) is in equilibrium with air temperature. In urban areas, commercial/industrial land use has high surface temperature values (ranges from 35.17 to 43.93°C) compared to low dense and high dense built-up which is mainly due to high activity level in those areas. The highest surface temperatures are observed over fallow lands (ranges from 39.08 to 51.98°C).

Figure 3 (a) and (b) show the spatial distribution of surface temperature of ASTER, dated October 18, 2001 at 11:18 Hrs. (day time) and of October 7, 2001 at 22:35 Hrs (night time). The estimated LST in day time ranges from 24.35°C to 54.29°C (mean value of 37.83°C and standard deviation of 4.235). It is observed that during day time fallow land exhibits the highest surface temperature from 41.16 to 53.09°C, followed by waste land/bare soil,

Table 3 Field measurements of emissivity in the 8–14 μm band for different samples

Date	Soil	Sparse vegetation	Dense vegetation	Urban (concrete)	Agricultural cropland (paddy)
October 4, 2005	0.923 ± 0.013	0.9560 ± 0.015	-	0.9156 ± 0.012	-
October 5, 2005	0.931 ± 0.014	-	0.9810 ± 0.006	-	0.9850 ± 0.013
October 6, 2005	-	0.9775 ± 0.016	0.9807 ± 0.012	0.9378 ± 0.014	0.987 ± 0.011
MEAN	**0.927 ± 0.013**	**0.9668 ± 0.015**	**0.9808 ± 0.09**	**0.9267 ± 0.013**	**0.9860 ± 0.013**

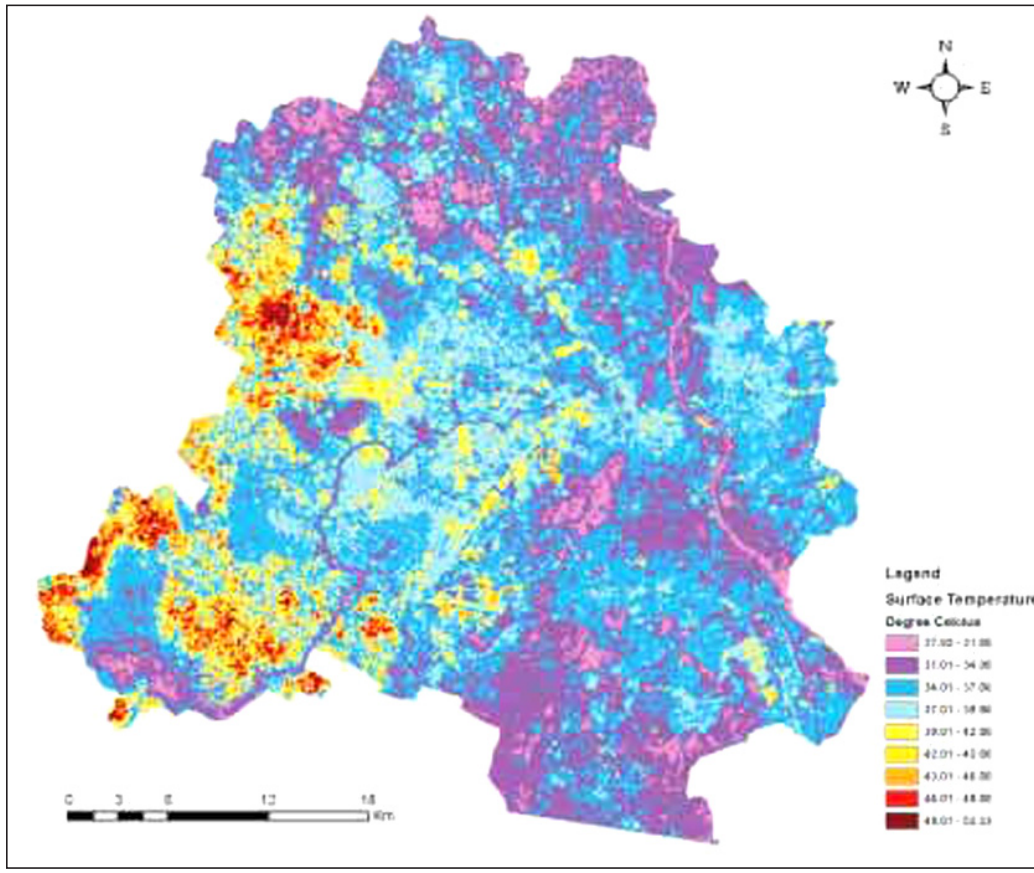

Fig. 2 Spatial distribution of land surface temperature over Delhi of ASTER, dated September 22, 2003.

commercial /industrial and high dense built-up, while water bodies, agricultural cropland, and dense vegetation shows low temperatures. Figure 4 shows the day time and night time mean thermal gradient of surface temperature over different LU/LC for the two ASTER datasets. The thermal gradient during day time increases from water bodies to fallow land, where as in the night time, mean thermal gradient decreases from high dense built-up to fallow land. In the surface temperature statistics of night time data the highest surface temperature is observed in high dense built-up, followed by water bodies, commercial/industrial and low dense built-up. Fallow land and waste land/bare soil due to low thermal capacity cools down faster than other LU/LC features. Hence fallow land, waste land/bare soil and sparse vegetation are cooler as compared to other LU/LC features during night time.

Relationship between vegetation density and land surface temperature

The relationship between the surface temperature of different LU/LC and vegetation density (NDVI and fraction vegetation cover) has been studied. The Pearson's correlation coefficients were computed between NDVI and FVC of each LU/LC and its surface temperature.

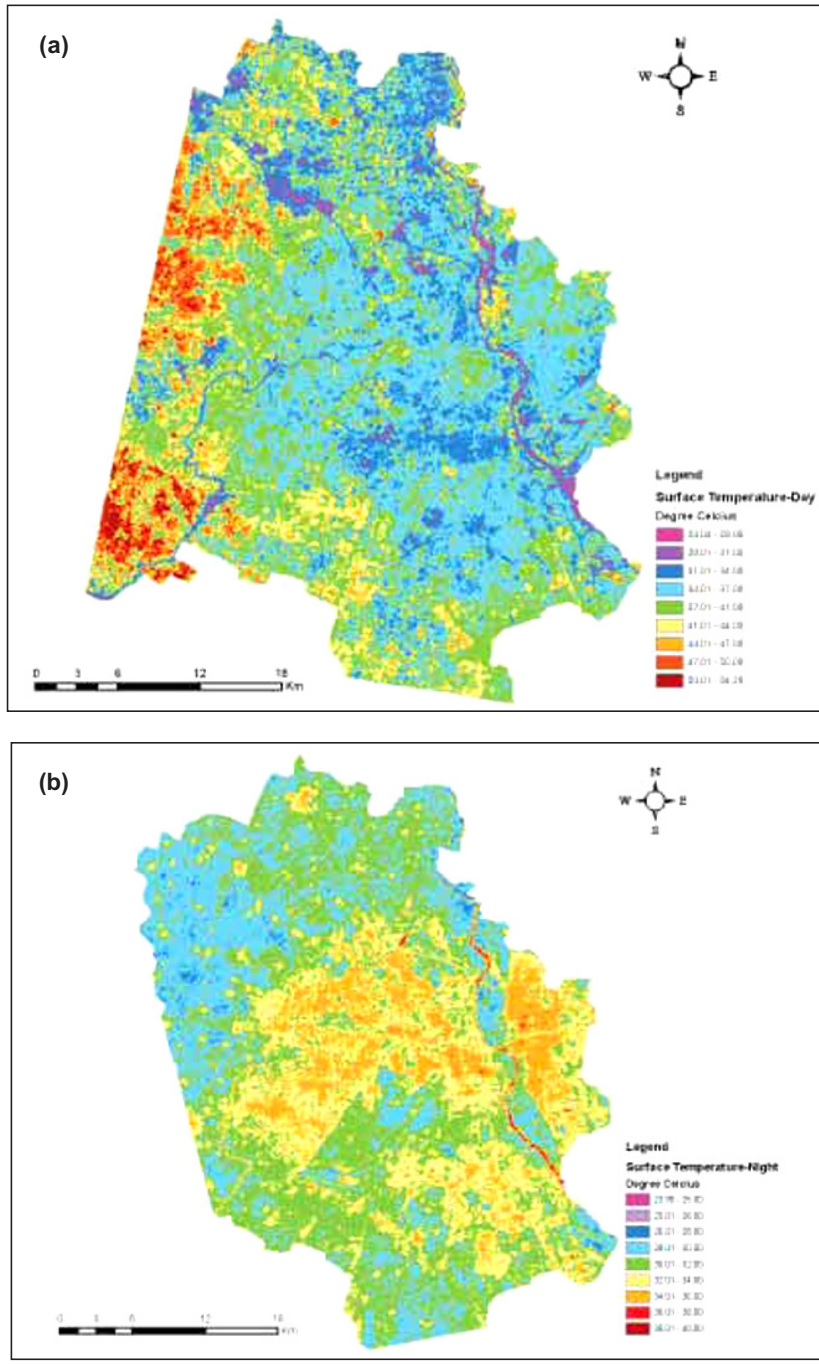

Fig. 3 Spatial distribution of surface temperature **(a)** ASTER, dated October 18, 2001 (day time) and **(b)** ASTER, dated October 7, 2001 (night time).

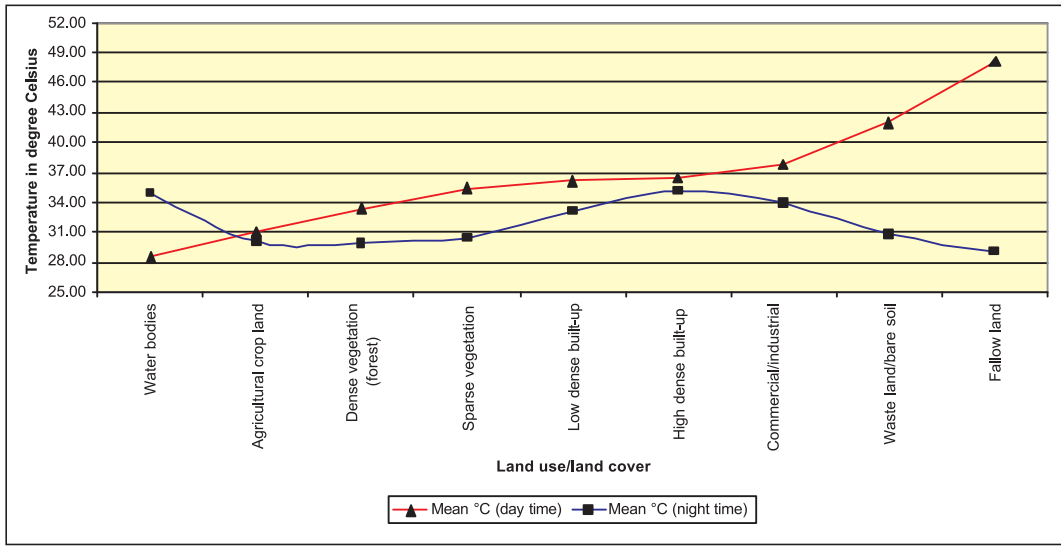

Fig. 4 Surface temperature of different Land use/land cover over Delhi of ASTER, dated October 18, 2001 (day time) and October 7, 2001 (night time).

NDVI values for ASTER data found to be from -0.128 to 0.714 (mean value of 0.317 and standard deviation of 0.145) for September 22, 2003 and from -0.059 to 0.633 (mean value of 0.249 and standard deviation of 0.091) for October 18, 2001 data. The FVC ranges from 0 to 1 indicating the vegetation abundance. The Pearson's correlation between surface temperature with NDVI and FVC for the entire image has been estimated and a negative correlation with NDVI (-0.581 for September 22, 2003 and -0.602 for October 18, 2001) as well as FVC (-0.475 for September 22, 2003 and -0.518 for October 18, 2001 respectively) were observed. For ASTER data night time (October 7, 2001), surface temperature has a negative correlation with NDVI (-0.451) and also for FVC (-0.447). Strong correlation between surface temperature with NDVI is observed over dense vegetation, sparse vegetation and low dense built-up for the two day time ASTER datsets and same trend is also found in FVC, which assures potential for using linear regression to predict surface temperatures if NDVI and fraction values are known. Regression coefficient between surface temperature with NDVI for dense vegetation (forest), sparse vegetation (park/grass), and low dense built-up with significance level of 0.01 was estimated. Regression coefficient between surface temperatures with NDVI for day time ASTER datsets (September 22, 2003 and October 18, 2001) are highest over dense vegetation (0.757 and 0.773), followed by sparse vegetation (0.657, 0.669) and low dense built-up (0.590, 0.405). Regression coefficient between surface temperatures with FVC was highest over dense vegetation (0.585, 0.500), followed by sparse vegetation (0.468, 0.479) and low dense built-up (0.362, 0.299) respectively. For ASTER night time data the correlation of surface temperature with NDVI and FVC has found to be low except for commercial/industrial (-0.541 for NDVI and -0.467 for FVC). Hence, the linear regression for night time image has not been considered.

Figure 5 shows the mean of surface temperature over different LU/LC using two night time ASTER datasets of October 7, 2001 and October 2, 2005. It is observed that the profile of surface temperature over LU/LC for both the datasets is similar. The mean surface temperature values for all LU/LC of October

2, 2005 are higher (0.5 to 1.6°C) to that of October 7, 2001. The differences may be due to acquisition of data in different time periods associated with external factors.

helpful in the studies leading to urban heat island (UHI) identification. It is inferred that the distribution of LU/LC favour the development of UHI not only as a difference in temperature between the city centre

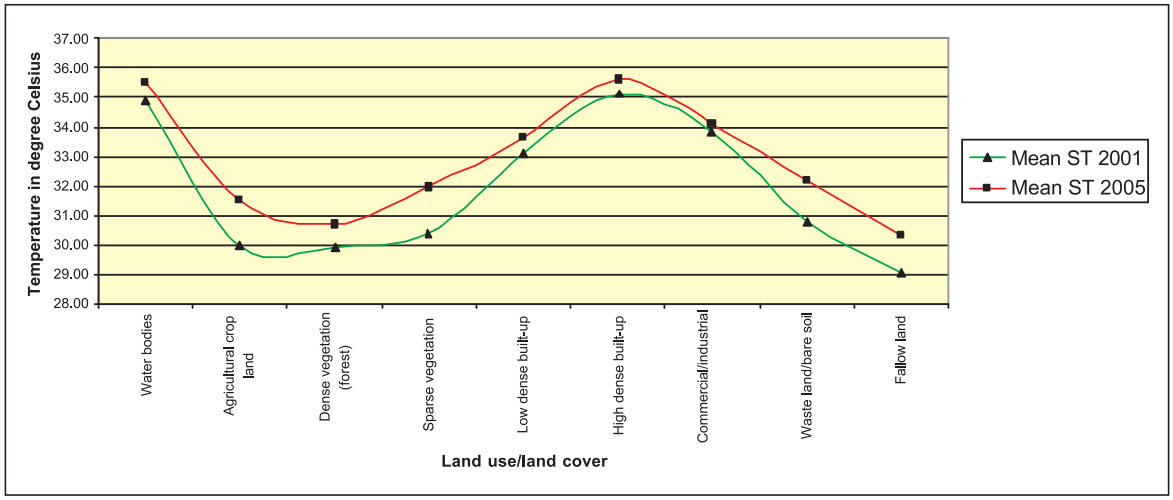

Fig. 5 Night time mean surface temperature of different Land use/land cover over Delhi of ASTER, dated October 2, 2005 and October 7, 2001.

In order to have the surface temperature pattern with different LU/LC in different zones of the areas, an attempt has been made to study the surface temperature along north–south and east–west transects so as to cover over different LU/LC. From the spatial profile of north–south transects it is seen that there are numerous 'peaks' from the centre of the city and decreases outwards (Fig. 6a). This is due to the fact that built-up and commercial/industrial areas are localized in the central area with low dense built-up and other LU/LC occurrences away from the centre. From the east–west transects pattern (Fig. 6b) it is evident that built up and commercial/industrial areas are more towards eastern part than western part. The spatial profile of north–south has higher thermal gradient while east–west has less thermal gradient, as the urban spread (built-up) is more towards east–west from centre than north to south. The spatial pattern of these LU/LC classes can be and its periphery but also among low dense built-up and commercial/industrial in the whole city, thus giving rise to the emergence of many small UHI throughout the study area.

Comparison of observed and estimated surface temperature

The acquisition of all the satellite datasets taken in the study were during the month of September and October. In order to compare the satellite estimated surface temperature values with the field measurements, a field campaign from October 3 – October 7, 2005 was carried out. During the campaign surface temperature measurements were taken during day and night for different features.

In the absence of field measurement in year 1999, 2001 and 2003 the estimated surface temperature values have been compared with those of the year

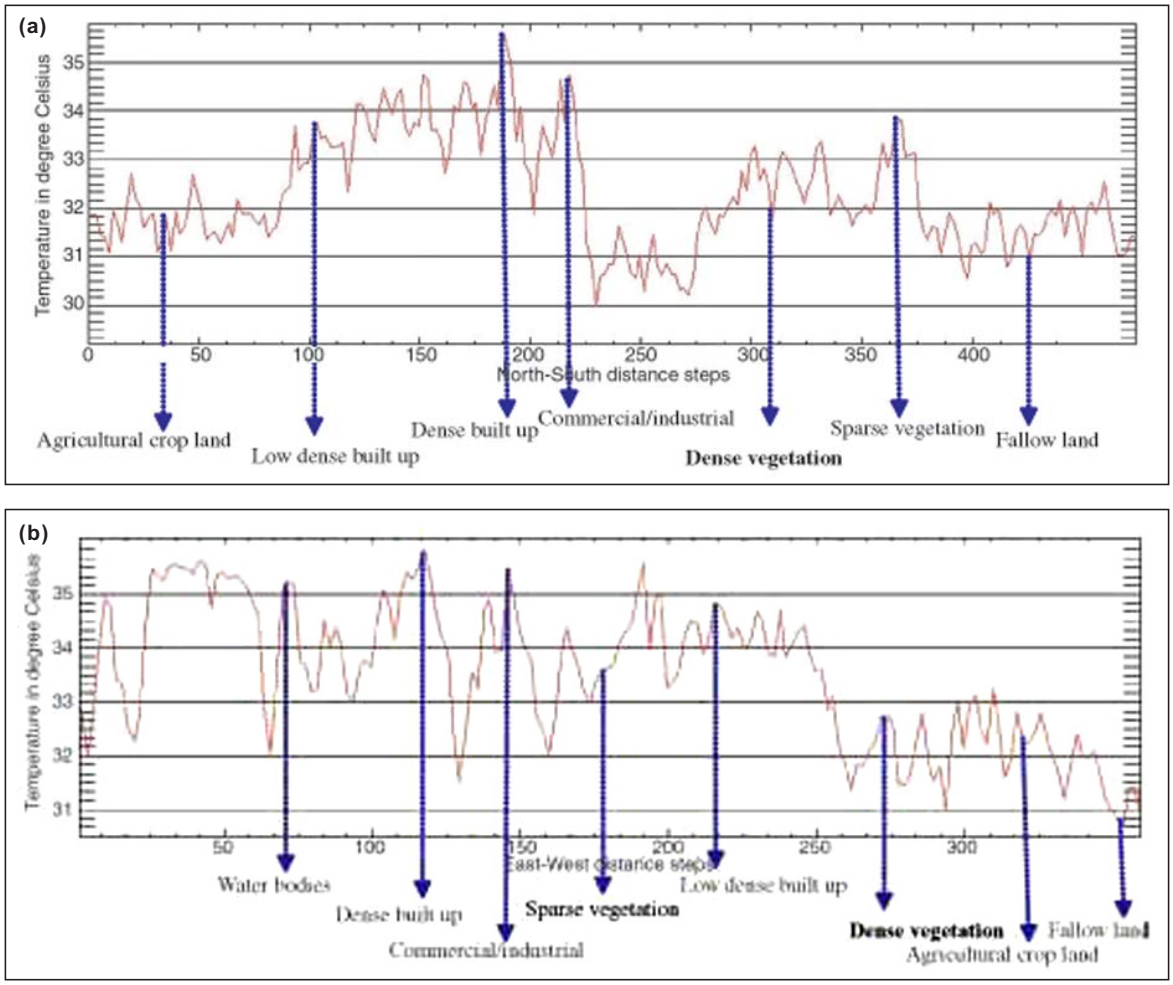

Fig. 6 Surface temperature profile along **(a)** North–south transect and **(b)** East–west transect for night time image of ASTER, dated October 2, 2005.

2005, maintaining the same period of season. Table 4, shows that the field values (night time measured LST) are in close comparison with those estimated using ASTER datasets. It is inferred that the errors in surface temperature estimation using satellite data are within the range of 3°C. To find out the difference between the temperatures on October 2 and October 3, 2005, ambient air temperature measurement were collected from Indian Meteorology department (IMD) at Safdarjung monitoring station, Delhi. The maximum and minimum air temperature values on October 2, 2005 were 34.2°C and 23.0°C respectively and on October 3, 2005 were 34.6°C and 21.5°C respectively which were appreciably close. Also a comparison of field measured surface temperature values with night time ASTER data dated October 7, 2001 reveals that the error in estimated surface temperature are within 3°C. Table 5 also shows the comparison between the satellites derived surface temperature values (day time ASTER 2001, 2003) and field measurement (day

Table 4 Comparison of satellite derived night time surface temperature with field measurement

Features	*In the field, observation on October 3, 2005 (21.30 to 23.00 local time) in °C	Satellite observation		UTM coordinates (meter)
		ASTER of October 7, 2001 (22.35 local time) in °C	ASTER of October 2, 2005 (22.35 local time) in °C	
Vegetation	28.50	29.64	31.10	718935 / 3159479
Vegetation	29.00	30.25	31.30	719570 / 3169243
Vegetation	29.30	30.67	31.47	718365 / 3167032
Vegetation	28.00	28.95	30.20	717613 / 3160398
Average	**28.70**	**29.88**	**31.02**	**-**
Bare soil	28.50	30.88	31.35	700395 / 3158756
Concrete (URBAN)	28.30	35.42	32.34	717811 / 3169012
Concrete (URBAN)	30.10	31.90	32.96	719871 / 3168740

*This measurement is the mean value 5 to 10 reading.

Table 5 Comparison of satellite derived day time surface temperature with field measurement

Features	*In the field observation on October 3–7, 2005 (10.30 to 12.00 local time) in °C	Satellite observation		UTM coordinates (meter)
		ASTER of October 7, 2001 in °C	ASTER of September 22, 2003 in °C	
Vegetation	33.20	32.58	31.99	711600 / 3168804
Vegetation	34.50	34.59	31.13	713443 / 3166854
Vegetation	34.25	32.36	35.07	715177 / 3164361
Vegetation	36.50	35.88	35.39	718428 / 3167288
Average	34.61	33.85	33.40	-
Bare soil	48.25	50.81	46.59	693503 / 3158835
Concrete (URBAN)	34.80	37.03	37.2	723630 / 3174656
Concrete (URBAN)	34.60	38.59	36.59	717275 / 3169419

* This measurement is the mean value 5 to 10 reading.

time), which also infers that the surface temperature values are in good agreement.

Conclusion

In this study, MNF components were used for classification which gives better classification accuracy than classification with original bands. Emissivity and surface temperature enables in better understanding of the overall urban land classes and in turn helps in understanding of energy budget issues. For estimation of emissivity, NDVI in conjunction with fraction vegetation cover at pixel level has been used and TES algorithm for ASTER

thermal bands for determination of LST. The estimated emissivity values over few LU/LC classes of ASTER data have been compared with the literature values and field measured values that showed promising results. The satellite derived surface temperature (day time and night time) has also been compared with field measured values (day time and night time) and found to be around ± 3ºC. Results show that the small increase in surface temperature at city level is mainly attributed due to cumulative impact of all changes in LU/LC and amount of vegetation. It is also seen that NDVI has better strong negative correlation than FVC with surface temperature which assures the potential to predict surface temperatures if NDVI values are known. Importance of FVC as an indicator of vegetation density has been examined. LU/LC level at city shows that high dense built-up, commercial/ industrial and low dense built-up has strong influences on surface temperature. Analysis of vegetation density with surface temperature has a low negative correlation at night time. The spatial layout of the LU/LC in the area has a great impact on the development of urban heat islands. Certain limitations encountered in this research work being non-availability of satellite datasets during summer season (May–June), where impact of surface temperature is felt maximum.

Acknowledgements This work has been conducted as a part of the IIRS-ITC joint educational/research program study. The authors acknowledge the Director, NRSC, Dean, IIRS, Rector, ITC for their encouragement and useful suggestions.

References

Champion HG and Seth SK (1968) A Revised Survey of Forest Types of India (New Delhi: Government of India Publication)

Gillespie AR (1985) Lithologic Mapping of Silicate Rocks Using TIMS Data Users' Workshop: *JPL Publication,* 86(38):29–44

Gillespie A, Shuichi R, Tsuneo M, Steven J, Simon H, and Anne K (1998) A temperature and emissivity separation algorithm for Advanced Space borne Thermal Emission and Reflection Radiometer (ASTER) images. *IEEE Transactions on Geosciences and Remote Sensing* 36(4):1113–1126

Kant Y and Badarinath KVS (2002) Ground based method for measuring thermal infrared effective emissivities: Implications and perpesctives on the measurement of land surface temperature from satellite data. *International Journal of Remote Sensing* 23(11): 2179–2191

Kaufmann YJ, Wald AE, Remer LA, Gao BC, Li RR and Flynn L (1997) The MODIS 2.µm Channel-Correlation with visible reflectance for use in remote sensing of aerosol. *IEEE Transactions on Geo-science and Remote Sensing* 35:1286–1298

Kustas WP and Norman JM (1996) Use of remote sensing for evapotranspiration monitoring over land surfaces. *Hydrological Sciences Journal* 41:495–516

Owe M and Van de Griend (1994) Ground based measurement on surface temperature and thermal emissivity. *Advances in Space Research* 14:45–58

Schmugge T, Hook SJ and Coll C (1998) Recovering surface temperature and emissivity from thermal infrared multispectral data. *Remote Sensing of Environment* 65:121–131

Wan Z, Zhang Y, Zhang Q and Li Z (2002) Validation of the land-surface temperature products retrieved from Terra Moderate Resolution Imaging Spectroradiometer data. *Remote Sensing of Environment* 83:163–180